《原子核物理评论》
www.npr.ac.cn Nuclear Physics Review
Started in 1984

致密物质中的pasta物相

申虹　胡金牛　纪凡　武旭浩　琚敏

Pasta Phases in Dense Matter

SHEN Hong, HU Jinniu, JI Fan, WU Xuhao, JU Min

在线阅读 View online: https://doi.org/10.11804/NuclPhysRev.41.QCS2023.02

引用格式:
申虹，胡金牛，纪凡，武旭浩，琚敏. 致密物质中的pasta物相[J]. 原子核物理评论，2024，41(3):811-817. doi: 10.11804/NuclPhysRev.41.QCS2023.02
SHEN Hong, HU Jinniu, JI Fan, WU Xuhao, JU Min. Pasta Phases in Dense Matter[J]. Nuclear Physics Review, 2024, 41(3):811-817. doi: 10.11804/NuclPhysRev.41.QCS2023.02

第 41 卷 第 3 期
2024 年 9 月

原 子 核 物 理 评 论
Nuclear Physics Review

Vol. 41, No. 3
Sep., 2024

Article ID: 1007-4627(2024)03–0811–07

Editors' Suggestion

Pasta Phases in Dense Matter

SHEN Hong[1], HU Jinniu[1], JI Fan[2,†], WU Xuhao[3,†], JU Min[4,†]

(*1. School of Physics, Nankai University, Tianjin 300071, China*;
2. National Key Laboratory of Particle Transport and Separation Technology, Tianjin 300180, China;
3. School of Science, Yanshan University, Qinhuangdao 066004, Hebei, China;
4. School of Science, China University of Petroleum (*East China*), *Qingdao 266580, Shangdong, China*)

Abstract: The pasta phases are expected to appear in hot supernova matter and cold neutron stars. In supernova matter, the pasta phases with a series of geometric shapes are studied using the compressible liquid-drop (CLD) model, where nuclear matter separates into a dense liquid phase of nucleons and a dilute gas phase of nucleons and α particles. The equilibrium conditions for two coexisting phases are derived by minimization of the total free energy including the surface and Coulomb contributions. Compared to the results considering only spherical nuclei, the inclusion of pasta phases can delay the transition to uniform matter and enlarge the region of nonuniform matter in the phase diagram. It is found that the density ranges of various pasta shapes depend on both the temperature and the proton fraction. The thermodynamic quantities obtained with the pasta phases using the CLD model are consistent with those in the realistic equation of state table for astrophysical simulations using the Thomas-Fermi approximation. The hadron-quark pasta phases occurring in the interior of massive neutron stars are studied using the energy minimization (EM) method, which is analogous to the CLD method for nuclear pasta. It was found that the hadron-quark pasta phases could be significantly affected by the model parameters used.

Key words: pasta phase; supernova matter; neutron star

CLC number: O571.6 **Document code:** A

DOI: 10.11804/NuclPhysRev.41.QCS2023.02 **CSTR:** 32260.14.NuclPhysRev.41.QCS2023.02

0 Introduction

Supernova explosions are spectacular astronomical events, which may lead to the formation of neutron stars or black holes[1]. The equation of state (EOS) of dense matter is an essential ingredient for understanding the dynamics of supernova explosions[2–4]. The supernova EOSs, which cover the wide range of temperature T, proton fraction Y_p, and baryon number density n_b (see, *e.g.*, Table 1 of Ref. [3]), exhibit a rich and complex phase diagram. At low temperatures and subsaturation densities, the matter is nonuniform where heavy nuclei are formed to lower the free energy of the system. When the density is beyond ~1/2 nuclear saturation density, heavy nuclei tend to dissolve into a uniform nucleon liquid. Some nonspherical nuclei, known as nuclear pasta phases, are expected to appear as the density approaches the phase transition to uniform matter[5–8]. At densities much higher than nuclear saturation density, non-nucleonic degrees of freedom like hyperons and quarks may occur and soften the EOS of dense matter[4]. The hadron-quark pasta phase, consisting of various geometries of mixed hadronic and quark matter, may occur during the deconfinement phase transition[9–11].

The appearance of pasta phase in dense matter is mainly caused by the competition between the surface and Coulomb energies. In nonuniform matter at subsaturation densities, the stable nuclear shape may change from droplet to rod, slab, tube, and bubble with increasing baryon density, which is also dependent on the nuclear model used[8]. Nuclear pasta phases are expected to occur both in core-collapse supernova matter with fixed proton fraction at finite temperature and in the inner crust of neutron stars where neutron-rich matter is in β equilibrium at zero temperature. Similar geometric structures, known as the hadron-quark pasta phases, may be formed in the core of massive neutron stars[12–13]. Generally, the Wigner-Seitz approximation with typical geometric shapes of pasta phases is employed to simplify the calculations. For more realistic description, there are some studies that have not explicitly assumed any geometric shape and performed fully three-di-

Received date: 27 Nov. 2023; **Revised date:** 19 Jun. 2024

Foundation item: National Natural Science Foundation of China (12175109)

Biography: SHEN Hong(1964−), female, Chengde, Hebei, Professor, working on nuclear astrophysics; E-mail: songtc@nankai.edu.cn

† **Corresponding author:** JI Fan, E-mail: jifan911@163.com; WU Xuhao, E-mail: yuechengflyingbird@qq.com; JU Min, E-mail: 15383088552@163.com

mensional calculations for nuclear pasta based on the Thomas-Fermi approximation[7, 14−15], Hartree-Fock approach[5, 16], and molecular dynamics method[6]. It is noteworthy that nuclear symmetry energy and its slope could significantly affect the pasta phase structure and crust-core transition of neutron stars[8].

This paper is arranged as follows. In Sect. 1, the pasta phases in hot supernova matter are studied using the compressible liquid-drop (CLD) method within the framework of the relativistic mean-field (RMF) approach. The phase diagram of nuclear pasta and its influence on the EOS are discussed. In Sect. 2, we explore the hadron-quark pasta phases appearing in the core of massive neutron stars using the energy minimization (EM) method, which is analogous to the CLD method used for describing nuclear pasta phases. Finally, the conclusions are presented in Sect. 3.

1 Pasta phases in supernova matter

We study the nuclear pasta phases in supernova matter with fixed proton fraction at finite temperature based on the CLD method, where the RMF model with extended TM1 parametrization (TM1e) is used for the nuclear interaction[17−18]. In the RMF approach, nucleons interact via the exchange of various mesons including the isoscalar-scalar meson σ, isoscalar-vector meson ω, and isovector-vector meson ρ. The nucleonic Lagrangian density can be found in Ref. [18].

We employ the CLD method to describe nuclear pasta phases, where the Wigner-Seitz approximation is adopted for simplifying the calculation of the free energy[19]. The nuclear matter inside the Wigner-Seitz cell is assumed to separate into a dense liquid (L) phase and a dilute gas (G) phase by a sharp interface, while the background electron gas is approximated to be uniform. The electron density is determined by the charge neutrality condition. At given temperature T, average baryon density $n_{\rm b}$, and proton fraction $Y_{\rm p}$, the equilibrium state can be determined by minimizing the total free energy density of the system among all configurations considered[2, 19]. The free energy density of the pasta phases is written as

$$f = uf^{L}\left(n_{\rm p}^{L}, n_{\rm n}^{L}\right) + (1-u) f^{G}\left(n_{\rm p}^{G}, n_{\rm n}^{G}, n_{\alpha}^{G}\right) + f_{\rm surf}(u, r_D, \tau) + f_{\rm Coul}\left(u, r_D, n_{\rm p}^{L}, n_{\rm p}^{G}, n_{\alpha}^{G}\right), \quad (1)$$

where u is the volume fraction of the liquid phase. The proton and neutron densities in the liquid (gas) phase are denoted by $n_{\rm p}^{L}$ ($n_{\rm p}^{G}$) and $n_{\rm n}^{L}$ ($n_{\rm n}^{G}$), respectively. The free energy contributed from nucleons in phase i ($i = L, G$) can be calculated within the RMF model[3, 20]. Note that contributions from electrons are not included in Eq. (1), since the background electron gas with a fixed density plays no role in the minimization procedure. Generally, the contributions from leptons and photons are treated separately when one constructs the EOS table for astrophysical simulations[3]. At finite temperature, the α particle is included as a representative light cluster in the dilute gas phase, whereas it is absent in the dense liquid phase. This is because the α particle tends to dissolve close to nuclear saturation density due to the finite volume effect[2−3]. For simplicity, the α particles are treated as noninteracting Boltzmann particles. In principle, other light clusters, such as deuterons, tritons, and helions may appear in supernova matter in addition to α particles. The appearance of these light clusters would modify the neutrino reaction rates, thereby influencing the supernova mechanism[4].

At given temperature T, average baryon density $n_{\rm b}$, and proton fraction $Y_{\rm p}$, we derive the equilibrium conditions between the liquid and gas phases by minimization of the total free energy including the surface and Coulomb contributions. The equilibrium equations are solved together with the coupled equations of the RMF model in the liquid and gas phases for all pasta shapes, and then the thermodynamically stable state is the one that has the lowest free energy density. For the nuclear interaction, we use the TM1e model with a small symmetry energy slope $L = 40$ MeV, which could be compatible with both experimental nuclear data and recent astrophysical observations. To examine the influence of the density dependence of symmetry energy, the results of the TM1e model are compared to those of the original TM1 model with a large symmetry energy slope $L = 110.8$ MeV. It is noteworthy that the TM1e and TM1 models have the same properties of symmetric nuclear matter but different density dependencies of symmetry energy, so that the comparison between the two models reflects the influence of the symmetry energy and its slope.

We first show in Fig. 1 the phase diagram of supernova matter including nuclear pasta in the $n_{\rm b}$-T plane for $Y_{\rm p} = 0.1$, 0.3, and 0.5 obtained in the TM1e model (left panels) compared to that in the TM1 model (right panels). The results with only droplet configuration are plotted by the dashed lines, so that the influence of nuclear pasta on the phase diagram can be examined. It is found that the inclusion of pasta phases delays the transition to uniform matter. This is because the configuration space is enlarged by considering nonspherical nuclei in addition to the droplet. It is shown that the density range of nonuniform matter depends on both T and $Y_{\rm p}$. At low temperatures, various pasta shapes appear one by one with increasing density, and the transition between different shapes is only weakly dependent on T. As T increases, the density range of nonuniform matter shrinks, and some pasta phases may disappear before the transition to uniform matter. By comparing the results of the TM1e model (left panels) to those of the TM1 model (right panels), one can see the influence of the symmetry energy slope on the phase diagram. It is

found that there is almost no difference in the case of $Y_p = 0.5$ and the difference for $Y_p = 0.3$ is still small. However, a significant difference between the TM1e and TM1 models is observed in the case of $Y_p = 0.1$. This is because the two models have the same isoscalar properties but different symmetry energy behavior. It is well known that the symmetry energy plays an important role in neutron-rich matter, but it has no impact on the properties of symmetric nuclear matter. A similar effect of the symmetry energy slope on the phase diagram was also reported in the literature, where the parametrized Thomas-Fermi approximation was used and only spherical nuclei were taken into account[18, 21]. The correlation between the symmetry energy slope L and the boundary of the liquid-gas coexistence region can be understood from the behavior of the pressure in asymmetric nuclear matter. It is well known that the pressure of pure neutron matter is approximately proportional to L. The TM1e model with a small symmetry energy slope $L = 40$ MeV yields relatively low pressures, particularly at lower Y_p values. Consequently, the upper boundary of its mechanically unstable region, characterized by negative compressibility, is located at higher densities. For further details, see Fig. 8 in Ref. [20].

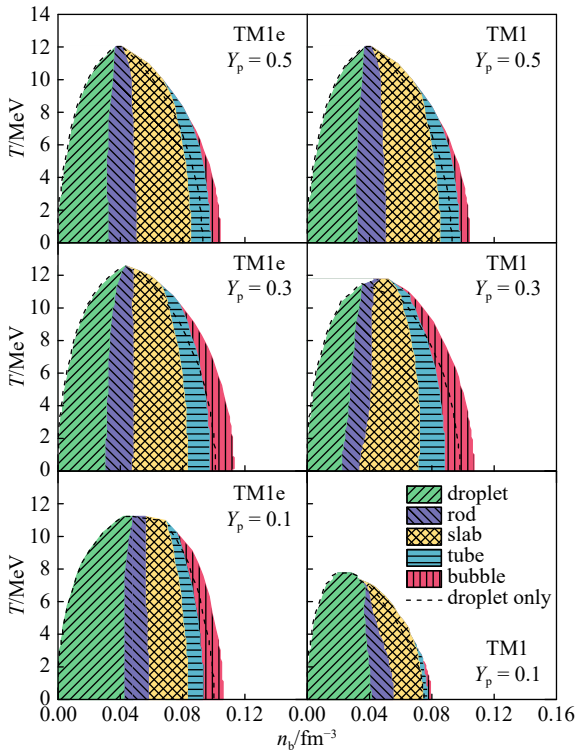

Fig. 1 (color online) Phase diagrams in the n_b - T plane for $Y_p = 0.1$, 0.3, and 0.5 obtained using the TM1e and TM1 models. Different colors indicate the regions for different pasta shapes. The boundary of nonuniform matter with only droplet configuration is shown by the dashed line for comparison.

In Fig. 2, the free energy per baryon, F, is plotted as a function of the baryon density n_b for $Y_p = 0.3$ at $T = 1$ and 10 MeV. The results with the inclusion of nuclear pasta (solid lines) are slightly smaller than those with droplet only (dashed lines) due to the enlargement of the configuration space by considering nonspherical nuclei. Meanwhile, the results from the realistic Shen EOS4[18], which were constructed using a parametrized Thomas-Fermi approximation with the TM1e model, are shown by dots for comparison. It is found that the values of F taken from the Shen EOS4 are very close to the results using the CLD method. This confirms that the two methods are consistent with each other for calculating the free energies. In Fig. 3, the pressure P is shown as a function of the baryon density n_b for $Y_p = 0.3$ at $T = 1$ and 10 MeV. Compared to the results with droplet only (dashed lines), small discontinuities are observed in the pressures with the inclusion of pasta phases (solid lines) due to the change of pasta shapes. The discontinuities exhibit the character of the first-order transition. It is found that the pressures taken from the Shen EOS4 are consistent with the results obtained using the CLD method. Note that the pressures depicted in Fig. 3 contain only the contributions of baryons, while the pressures from leptons and photons are treated separately, according to tradition for constructing the EOS table. In the case of $T = 1$ MeV and $Y_p = 0.3$, the pressure decreases with increasing density and can even reach negative values. This is because the pressure of electrons is significantly higher than that of baryons in this case, and the total pressure becomes positive

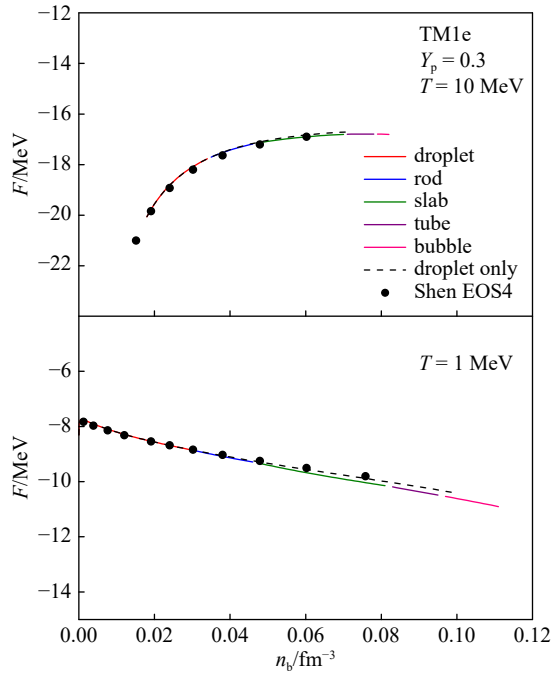

Fig. 2 (color online) Free energy per baryon F as a function of the baryon density n_b for $Y_p = 0.3$ at $T = 1$ and 10 MeV using the TM1e model. The results with nuclear pasta (solid lines) are compared to those with droplet only (dashed lines). The dots represent the values from the Shen EOS4, which were obtained by a parameterized Thomas-Fermi approximation[18].

when the contributions from electrons are taken into account.

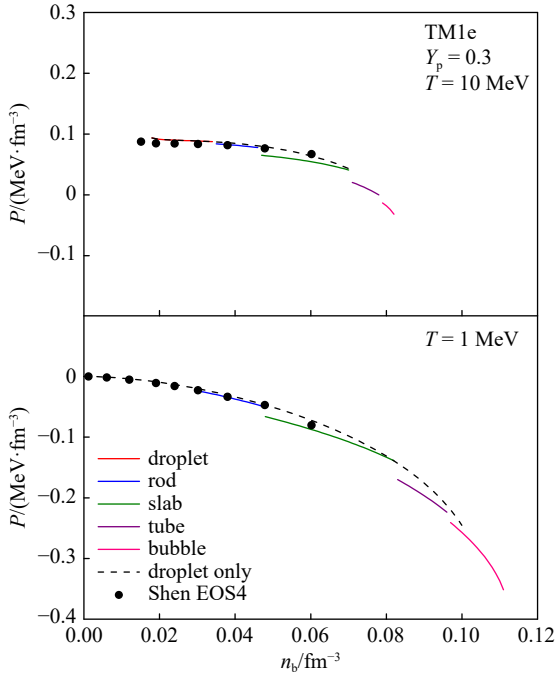

Fig. 3 (color online) Same as Fig. 2, but for pressure P.

2 Hadron-quark pasta phases in neutron stars

In the core of massive neutron stars, exotic phases like deconfined quarks may be present. During the deconfinement phase transition, some geometric structures, known as hadron-quark pasta phases, may be formed[9−13, 22]. This structured mixed phase is analogous to nuclear pasta occurring at subsaturation densities. Several methods have been developed to study the properties of hadron-quark pasta phases. In the coexisting phases (CP) method[12], the hadronic and quark phases are assumed to satisfy the Gibbs conditions for phase equilibrium, while the surface and Coulomb energies are taken into account perturbatively. A more realistic description of the pasta phase has been developed in a series of works[9−10], where the Thomas-Fermi approximation was used to describe the density profiles of hadrons and quarks in the Wigner-Seitz cell. In our previous works[12−13], we proposed an energy minimization (EM) method for improving the treatment of surface and Coulomb energies, which play a key role in determining the structure of the pasta phases. By incorporating the surface and Coulomb contributions in the EM procedure, one can derive the equilibrium conditions between the two coexisting phases. The basic idea of the EM method for the hadron-quark pasta phase is very similar to that of the CLD method for nuclear pasta. In the EM method, the Wigner-Seitz approximation is adopted for simplifying the calculations, where the whole space is divided into equivalent cells with a geometric symmetry. The coexisting hadronic and quark phases in a charge-neutral cell are assumed to be separated by a sharp interface, while the particle densities in each phase are taken to be uniform. The surface tension at the interface plays a crucial role in determining the structure of the mixed phase, which is generally treated as a free parameter.

In the EM method, the total energy density of the hadron-quark mixed phase is written as

$$\varepsilon_{\rm MP} = \chi\varepsilon_{\rm QP} + (1-\chi)\varepsilon_{\rm HP} + \varepsilon_{\rm surf} + \varepsilon_{\rm Coul}, \tag{2}$$

where $\chi = V_{\rm QP}/(V_{\rm QP}+V_{\rm HP})$ denotes the volume fraction of the quark phase. The energy density of the hadronic matter, $\varepsilon_{\rm HP}$, is calculated in the RMF model. Meanwhile, the energy density of the quark matter, $\varepsilon_{\rm QP}$, can be obtained using the MIT bag model or the Nambu-Jona-Lasinio (NJL) model with the inclusion of repulsive vector interactions. The vector coupling $G_{\rm V}$ is treated as a free parameter, since there is still no constraint on $G_{\rm V}$ at finite density. Further details on the vector interactions can be found in Wu *et al.*[12] for the NJL model, and in Ju *et al.*[13] for the modified MIT bag model.

During the hadron-quark phase transition, several pasta configurations may appear in the order of droplet, rod, slab, tube, and bubble with increasing density. The results are influenced by both methods used and model parameters. In Fig. 4, we show the density ranges of various pasta shapes as a function of the surface tension σ. The results obtained from the EM and CP methods are displayed in the upper and lower panels, respectively. One can see that the onsets of all pasta shapes in the CP method are independent of σ. This is because the equilibrium state in the CP method is determined by the Gibbs conditions. The surface tension σ does not influence the Gibbs phase equilibrium equations, which require that pressures and chemical potentials should be equal between the two phases. However, the dependence on the surface tension σ in the EM method is much more complicated, since the finite-size effects have been included in the equilibrium conditions. Therefore, the transition density obtained in the EM method is clearly dependent on σ as shown in the upper panels of Fig. 4. As σ increases, the density range of hadron-quark mixed phase significantly shrinks and the number of pasta configurations is reduced. By comparing the left and right panels, one can see that the repulsive vector interactions in the NJL model can significantly push the mixed phase toward higher densities with a wider range. This is attributed to the fact that the inclusion of repulsive vector interactions causes a corresponding increase in the energy and pressure of quark matter. Similar effects of the vector coupling on the mixed phase are also observed in the following figures using a modified MIT bag model for quark matter.

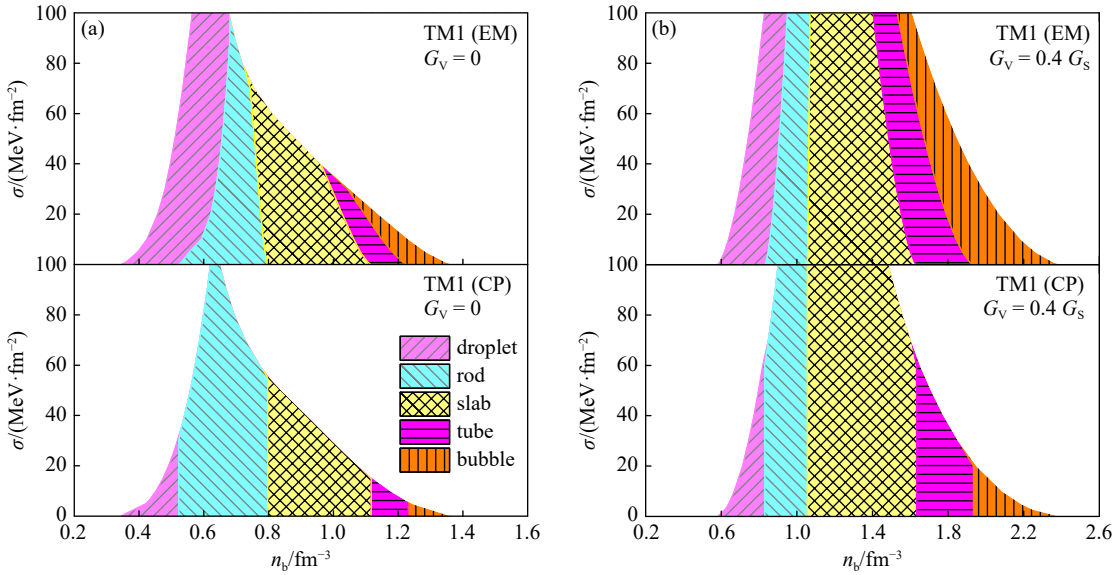

Fig. 4 (color online) Density ranges of various pasta shapes as a function of the surface tension σ. The results obtained using the EM and CP methods are displayed in the upper and lower panels, respectively. The results with a repulsive vector interaction ($G_V = 0.4 G_S$) in right panel are compared to those without vector interaction ($G_V = 0$) in left panel.

To analyze the influence of the vector coupling G_V on the deconfinement phase transition, it is convenient to use the Maxwell construction in which the phase transition appears at the crossing of the hadronic EOS with the quark EOS in the pressure and chemical potential plane. This is due to that two coexisting phases in the Maxwell construction must have the same pressure and baryon chemical potential. In Fig. 5, we plot the pressure P as a function of the neutron chemical potential μ_n. The hadronic matter is calculated using the RMF model with the BigApple parametrization, while the quark matter is described by a modified MIT bag model with the bag constant $B^{1/4} = 180$ MeV and different vector coupling G_V. One can see that a larger G_V in the bag model corresponds to a higher transition pressure, which implies that the deconfinement phase transition is delayed accordingly. Therefore, the formation of hadron-quark pasta phases may be delayed with increasing vector coupling G_V in the bag model. In Fig. 6, we show the pressure P as a function of the baryon density n_b for hadronic, mixed, and quark phases. The calculations of the hadron-quark pasta are performed in the EM method, where the hadronic matter is described by the BigApple model and the quark matter by the bag model with $B^{1/4} = 180$ MeV. For comparison, the results of the Gibbs and Maxwell constructions are displayed by red solid and green dotted lines, respectively. It is shown that the results of pasta phases lie between the Gibbs and Maxwell constructions. As the vector coupling G_V increases from left to right panels, one can see that the hadron-quark mixed phases appear at higher densities and pressures.

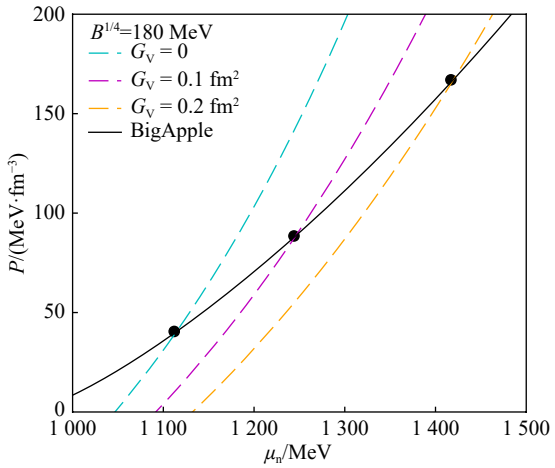

Fig. 5 (color online) Pressure P as a function of the neutron chemical potential μ_n. The hadronic matter is calculated by the RMF model with the BigApple parametrization. The quark matter is described by a modified MIT bag model with the bag constant $B^{1/4} = 180$ MeV and different vector coupling G_V. The filled circles indicate the crossing points of the hadronic and quark curves corresponding to the phase transition in the Maxwell construction.

In Fig. 7, we display the predicted mass-radius relations of neutron stars, together with several constraints from astrophysical observations. Compared to the results using pure hadronic EOS (solid lines), the inclusion of hadron-quark pasta phases leads to an obvious reduction of the maximum neutron-star mass M_{max}. The hadron-quark pasta phases are taken into account by using the EM method. The results of massive neutron stars are strongly dependent on the vector coupling G_V in the bag model. It is found that both the onset of hadron-quark pasta phases (filled circles) and the values of M_{max} (filled squares) increase with increasing G_V.

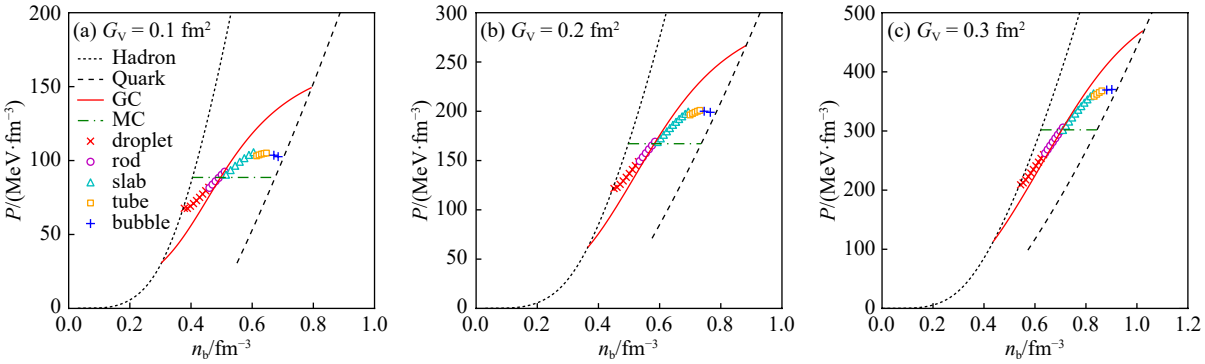

Fig. 6 (color online) Pressure P as a function of the baryon density n_b for hadronic, mixed, and quark phases. The hadronic matter is calculated by the RMF model with the BigApple parametrization. The quark matter is described by a modified MIT bag model with the bag constant $B^{1/4} = 180$ MeV for several vector coupling G_V. The results of pasta phases obtained using the EM method are compared to those of the Gibbs construction (GC) and Maxwell construction (MC).

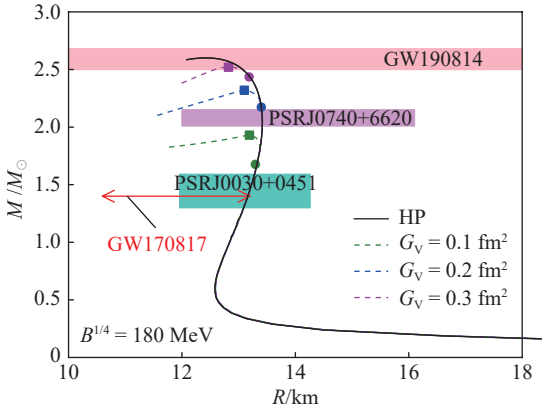

Fig. 7 (color online) Mass-radius relations of neutron stars for different model parameters. The results of the pure hadronic EOS are compared to those including the hadron-quark mixed phase described in the EM method for different vector coupling G_V. The red horizontal line with arrows at both ends represents the constraint on $R_{1.4}$ inferred from GW170817[23]. The green and purple shaded areas correspond to simultaneous measurements of the mass and radius from NICER for PSR J0030+0451[24] and PSR J0740+6620[25], respectively. The mass constraint from GW190814[26] is depicted by the pink horizontal bar.

3 Conclusions

The pasta phases may occur in hot supernova matter and cold neutron stars. We studied nuclear pasta phases appearing in supernova matter at subsaturation densities by using the CLD method, where nuclear matter separates into a dense liquid phase and a dilute gas phase. Meanwhile, the equilibrium conditions for two coexisting phases were derived by minimization of the total free energy including the surface and Coulomb contributions. It was found that the inclusion of pasta phases can delay the transition to uniform matter and enlarge the region of nonuniform matter in the phase diagram. The thermodynamic quantities such as the free energy and pressure obtained with the pasta phases in the CLD model are consistent with those in the realistic EOS table by the Thomas-Fermi approximation. It was shown that the nuclear symmetry energy and its density dependence play a crucial role in determining the properties of pasta phases in neutron-rich matter.

The hadron-quark pasta phases occurring in the interior of massive neutron stars were studied using the EM method, where the surface and Coulomb contributions are included in the energy minimization procedure, which is analogous to the CLD method for nuclear pasta phases at subsaturation densities. The hadronic matter is described in the RMF model, while the quark matter can be described using the MIT bag model or the NJL model with the inclusion of repulsive vector interactions. It was found that the hadron-quark pasta phases could be significantly affected by the model parameters used. A larger vector coupling G_V predicts that the hadron-quark pasta phases appear at higher densities, and as a result, the reduction of M_{max} due to quarks is smaller.

References:

[1] BURROWS A. Rev Mod Phys, 2013, 85: 245.
[2] LATTIMER J M, SWESTY F D. Nucl Phys A, 1991, 535(2): 331.
[3] SHEN H, TOKI H, OYAMATSU K, et al. The Astrophysical Journal Supplement Series, 2011, 197(2): 20.
[4] OERTEL M, HEMPEL M, KLÄHN T, et al. Rev Mod Phys, 2017, 89: 015007.
[5] PAIS H, STONE J R. Phys Rev Lett, 2012, 109: 151101.
[6] WATANABE G, SONODA H, MARUYAMA T, et al. Phys Rev Lett, 2009, 103: 121101.
[7] OKAMOTO M, MARUYAMA T, YABANA K, et al. Phys Rev C, 2013, 88: 025801.
[8] BAO S, SHEN H. Phys Rev C, 2015, 91: 015807.
[9] MARUYAMA T, CHIBA S, SCHULZE H J, et al. Phys Rev D, 2007, 76: 123015.
[10] YASUTAKE N, ŁASTOWIECKI R, BENIĆ S, et al. Phys Rev C, 2014, 89: 065803.
[11] WEBER F, FARRELL D, SPINELLA W M, et al. Universe, 2019, 5(7): 169.
[12] WU X, SHEN H. Phys Rev C, 2019, 99: 065802.
[13] JU M, HU J, SHEN H. The Astrophysical Journal, 2021, 923(2):

250.
[14] JI F, HU J, SHEN H. Phys Rev C, 2021, 103: 055802.
[15] XIA C J, MARUYAMA T, YASUTAKE N, et al. Phys Lett B, 2023, 839: 137769.
[16] FATTOYEV F J, HOROWITZ C J, SCHUETRUMPF B. Phys Rev C, 2017, 95: 055804.
[17] BAO S, HU J, ZHANG Z, et al. Phys Rev C, 2014, 90: 045802.
[18] SHEN H, JI F, HU J, et al. The Astrophysical Journal, 2020, 891(2): 148.
[19] JI F, HU J, BAO S, et al. Phys Rev C, 2020, 102: 015806.
[20] BAO S, SHEN H. Phys Rev C, 2016, 93: 025807.
[21] TOGASHI H, NAKAZATO K, TAKEHARA Y, et al. Nucl Phys A, 2017, 961: 78.
[22] WU X, SHEN H. Phys Rev C, 2017, 96: 025802.
[23] ABBOTT B P, ABBOTT R, ABBOTT T, et al. Phys Rev Lett, 2018, 121: 161101.
[24] MILLER M C, LAMB F K, DITTMANN A J, et al. The Astrophysical Journal Letters, 2019, 887(1): L24.
[25] MILLER M C, LAMB F K, DITTMANN A J, et al. The Astrophysical Journal Letters, 2021, 918(2): L28.
[26] ABBOTT R, ABBOTT T, ABRAHAM S, et al. The Astrophysical Journal Letters, 2020, 896(2): L44.

致密物质中的 pasta 物相

申 虹[1], 胡金牛[1], 纪 凡[2,†], 武旭浩[3,†], 琚 敏[4,†]

(1. 南开大学物理科学学院，天津 300071；
2. 粒子输运与富集技术全国重点实验室，天津 300180；
3. 燕山大学理学院，河北 秦皇岛 066004；
4. 中国石油大学(华东)理学院，山东 青岛 266580)

摘要： Pasta 物相有可能出现在热的超新星物质和冷中子星中。在超新星物质中，具有一系列几何形状的 pasta 物相可以采用可压缩液滴(CLD)模型研究，其中核物质被划分为核子的致密液相和核子的稀薄气相。通过最小化包括表面能和库仑能贡献的总自由能，可以推导出两相共存的平衡条件。与仅考虑球形核的结果相比，包括 pasta 物相可以延迟向均匀物质的相变并扩大相图中的非均匀物质区域。研究发现，各种 pasta 形状的密度范围依赖于温度和质子分支比。采用 CLD 模型描述 pasta 物相所得到的热力学量与采用 Thomas-Fermi 近似得到的用于天体物理数值模拟的现实状态方程表中的热力学量基本一致。另一方面，采用能量最小化(EM)方法研究了可能发生在大质量中子星内部的强子-夸克 pasta 物相，该方法类似于 CLD 方法用于研究核的 pasta 物相。研究发现，采用的模型参数对于强子-夸克 pasta 物相有显著影响。

关键词： pasta 物相；超新星物质；中子星

收稿日期: 2023-11-27；　**修改日期:** 2024-06-19
基金项目: 国家自然科学基金资助项目(12175109)
† **通信作者:** 纪凡, E-mail: jifan911@163.com；武旭浩, E-mail: yuechengflyingbird@qq.com；琚敏, E-mail: 15383088552@163.com